Bulletin of the Seismological Society of America, Vol. 96, No. 4B, pp. S28–S37, September 2006, doi: 10.1785/0120050824

San Andreas Fault Geometry in the Parkfield, California, Region

by R. W. Simpson, M. Barall, J. Langbein, J. R. Murray, and M. J. Rymer

Abstract In map view, aftershocks of the 2004 Parkfield earthquake lie along a line that forms a straighter connection between San Andreas fault segments north and south of the Parkfield reach than does the mapped trace of the fault itself. A straightedge laid on a geologic map of Central California reveals a ~50-km-long asymmetric northeastward warp in the Parkfield reach of the fault. The warp tapers gradually as it joins the straight, creeping segment of the San Andreas to the northwest, but bends abruptly across Cholame Valley at its southeast end to join the straight, locked segment that last ruptured in 1857. We speculate that the San Andreas fault surface near Parkfield has been deflected in its upper ~6 km by nonelastic behavior of upper crustal rock units. These units and the fault surface itself are warped during periods between large 1857-type earthquakes by the presence of the 1857-locked segment to the south, which buttresses intermittent coseismic and continuous aseismic slip on the Parkfield reach. Because of nonelastic behavior, the warping is not completely undone when an 1857-type event occurs, and the upper portion of the three-dimensional fault surface is slowly ratcheted into an increasingly prominent bulge. Ultimately, the fault surface probably becomes too deformed for strike-slip motion, and a new, more vertical connection to the Earth's surface takes over, perhaps along the Southwest Fracture Zone. When this happens a wedge of material currently west of the main trace will be stranded on the east side of the new main trace.

Introduction

Chinnery (1966), Bridwell (1975), and other modelers have remarked upon the tendency for the ends of slipping dislocation patches in an elastic medium to rotate: Ends of an isolated right-lateral slipping patch tend to rotate counterclockwise when viewed from above. This rotation is accommodated by deformation in the adjacent elastic material. In a perfectly elastic medium if in-line patches adjacent to the slipping patch are also allowed to slip, the fault formed by these patches will unrotate and revert to its original straight geometry. Bridwell (1975) pointed out that deformation cycles of this sort, coupled with nonelastic behavior in the adjacent rocks, could, over the long term, produce the sinuous pattern of fault traces observed on geologic maps. He described a finite-element model simulating the coseismic distortion of the fault plane during Parkfield earthquakes.

Hypocenters of relocated aftershocks of the 2004 Parkfield earthquake (Thurber *et al.*, 2006) lie mostly to the southwest of the mapped trace of the creeping San Andreas fault in the Parkfield region, and more directly under the trace of the Southwest Fracture Zone (Figs. 1 and 2). (The words "southwest" and "northeast" are used in this article to signify fault-perpendicular directions—more exactly S50°W and N50°E.) In map view, the aftershocks define a trend that forms a straighter connection between the San Andreas segments to the north and south of the Parkfield reach than does the mapped trace of the fault itself. This trend can also be seen in the distribution of 1966 aftershocks located by Eaton *et al.* (1970) and in the relocation of Parkfield background seismicity using a three-dimensional (3D) velocity model by Eberhart-Phillips and Michael (1993).

Many investigators have noted the presence of a right-stepping offset of the main active trace of the San Andreas fault across Cholame Valley south of Parkfield (e.g., Brown *et al.*, 1967; Brown, 1970; Sibson, 1986). (See figure 1 of Rymer *et al.* [2006].) This right offset is thought to lie at the approximate location of the north end of the locked zone that last ruptured in the **M** 7.9 Fort Tejon earthquake in 1857 (Sieh, 1978). Farther to the northwest along the fault, near the epicenter of the 1966 Parkfield earthquake, Lindh and Boore (1981) have pointed out the existence of a 5° bend in the fault trace near the common epicenter of the 1934 and 1966 **M** ~ 6.0 Parkfield earthquakes. Several researchers have mentioned the offset and the bend in broader discussions of the effects of fault geometry upon the concentration of stress and the location of earthquakes (e.g., Segall and Pollard, 1980; King and Nabelek, 1985). Bridwell (1975) proposed that Parkfield earthquakes themselves could be re-

Figure 1. Map showing the San Andreas fault in central California. Rectangular box shows the location of Figure 2. LO, Logan Quarry; GH, Gold Hill; CV, Cholame Valley; ERP, Eagle Rest Peak.

sponsible for the observed fault geometry at the Earth's surface.

The models described below and geologic considerations suggest (1) that the offset and the bend in the fault trace near Parkfield may be more fruitfully regarded as parts of an asymmetric 3D warp or bulge in the upper part of the fault surface, (2) that the warp may be a consequence of the 1857-locked patch that exists south of Cholame Valley combined with nonelastic behavior in adjacent rock units, and (3) that the warp may grow with time until a new straighter trace eventually breaks through to the surface, perhaps along the Southwest Fracture Zone.

The warp extends from approximately 15 km southeast of Gold Hill to approximately 30 km northwest. Its surface manifestation can be viewed in a broader context with the help of a straightedge and a regional geologic map such as Jennings (1977). The southeastern end of the warp in Cholame Valley is more abruptly curved than the northwestern end, which tapers gradually into the creeping section of the San Andreas north of Middle Mountain. Figure 3 shows a surface constructed by interpolation and extrapolation from the aftershocks of the 2004 earthquake and the mapped creeping trace of the San Andreas fault.

We propose that the first-order features of the warp are caused by the presence of the 1857-locked patch, although second-order features, including perhaps the 5° bend, might be cause by the locked patch (or patches) that fail in Parkfield-type events. We also remark that "nonelastic behavior"

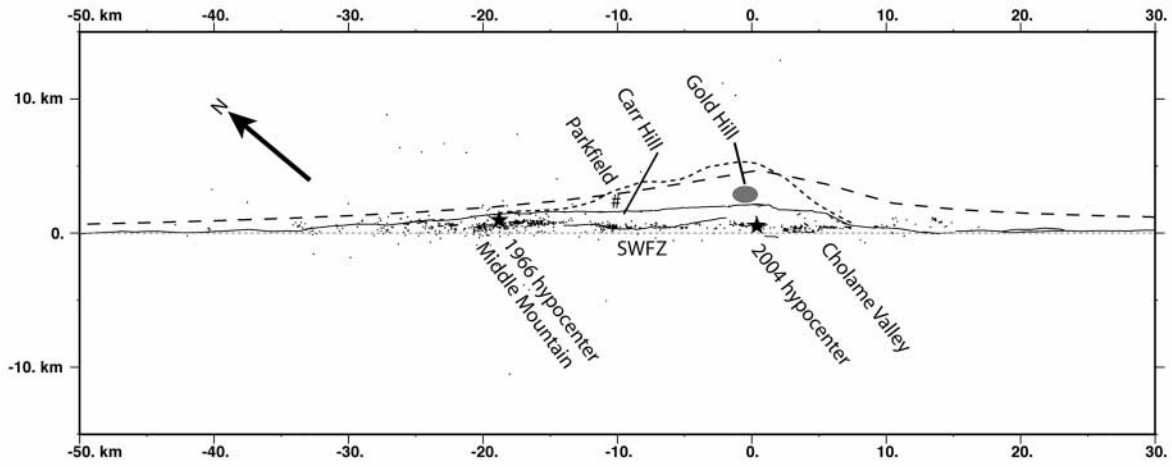

Figure 2. Oblique Mercator projection showing selected faults and 2004 aftershocks (Thurber *et al.*, 2006) below 6 km depth in the vicinity of Parkfield. The equator of the projection (thin straight dashed line) passes near the 2004 epicenter (small star) at an azimuth of N40°W. The solid continuous line is the active San Andreas fault trace and the short dashed line is an old San Andreas fault trace behind Gold Hill, as mapped by Dibblee (Dibblee *et al.*, 1999, 2004). The disconnected lines southwest of the active trace are Alquist–Priolo fault traces and the Southwest Fracture Zone trace (Brown *et al.*, 1967; Brown, 1970). The long dashed line shows the predicted deflection of a line 2.5 km northeast of the dislocation model fault trace after one million years in the absence of 1857-type earthquakes.

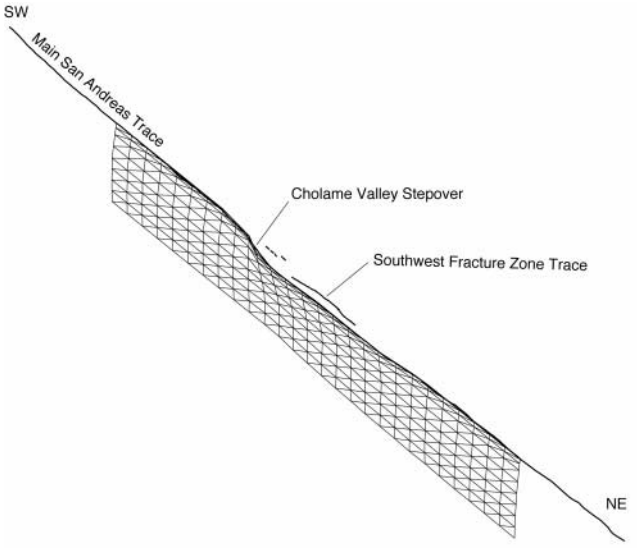

Figure 3. View looking down and toward the south at a representation of the current active fault surface. The surface was defined by interpolating and extrapolating between hypocenters of relocated earthquakes from 1984 to 2005 (Thurber *et al.*, 2006) and the San Andreas trace at the Earth's surface mapped by Dibblee (solid continuous line at top). Horizontal lines in the fault surface are at 0.85-, 2-, 4-, 6-, 8-, 10-, 12-, and 14-km depth.

might not be limited to classical plastic or viscoelastic rheologies, but could also include other effects like slip along near-horizontal faults. In the following sections, we present geologic, geodetic, and seismologic observations that, we think, support our hypothesis. We also describe a simple dislocation model and some preliminary finite-element modeling efforts that confirm, at least in a qualitative way, the possibility of finding model rheologies that could produce the postulated warping. Finally, assuming that the process of warping has persisted for some time in the Parkfield region, we consider some possible implications.

Geologic Observations

Mafic igneous rocks exposed at Gold Hill on the northeast side of the current creeping San Andreas trace have lithologic similarities with igneous rocks at Eagle Rest Peak in the San Emigdio Mountains (Fig. 1) about 150 km to the southeast (Ross, 1984; Sims, 1993). The rocks at Gold Hill are thought to have been carried to the north from Eagle Rest Peak as part of the Pacific Plate. The presence near Parkfield of these exotic, far-traveled rocks, which now lie on the wrong side of the San Andreas fault, is consistent with geologic observations of Dickinson (1966), who described faults to the northeast of Gold Hill that he identified as former, now inactive strands of the San Andreas system that have been bulged northeastward with time. Mapped structures and reverse faults east of Gold Hill are also consistent with a northeast warping of the units exposed at the surface (Dickinson, 1966; Thayer *et al.*, 2004; C. Wentworth, personal comm., 2005). The dense magnetic gabbro that forms Gold Hill allows an estimate of its size and depth extent from potential field modeling of associated gravity and aeromagnetic anomalies. It appears that the gabbro forms a fault-bounded sliver that most likely does not extend to very great depth (McPhee *et al.*, 2004).

If a new, straighter trace, perhaps along the Southwest Fracture Zone, does eventually take over from the current main trace, a wedge of material currently on the west side of the San Andreas will again become stranded on the east side, as appears to have happened at least once before when Gold Hill was stranded.

Earthquake Hypocenters

Eaton *et al.* (1970) fitted a plane through their best located 1966 aftershocks. The plane had a strike of N39°W with a dip of 86°SW, although it appears that events below 5–6 km could be equally well fitted by a vertical plane. The distribution of their 1966 aftershock locations is consistent with the geometry of our proposed warp.

Thurber *et al.* (2006) have relocated aftershocks of the 2004 Parkfield earthquake and preearthquake seismicity occurring between 1984 and 2004 using a new 3D wavespeed model and the double-difference relocation technique. Events falling below 6-km depth can be fitted (with some scatter) by a relatively simple, nearly vertical surface that projects upward to a line at the Earth's surface lying several kilometers to the southwest of the mapped, creeping main trace of the San Andreas fault (Figs. 2 and 4). These events lie more directly under the Southwest Fracture Zone than under the main trace. Events above 6-km depth are mostly contained in an envelope formed by two surfaces that diverge at 6-km depth and rise to meet these two separate surface traces. In one location, when viewed in cross section, there are aftershocks on two distinct branching strands forming a Y shape (Fig. 5) (Bakun *et al.*, 2005, their figure 2f). There are not enough earthquakes at shallow depths to make a definitive connection between these branching strands and surface traces, but postseismic afterslip (Lienkaemper *et al.*, 2006; Murray and Langbein, 2006; Rymer *et al.*, 2006) on the main trace would seem to indicate that deep coseismic slip has made its way to the surface along the main strand. (Coseismic offset observed on the Southwest Fracture Zone [Langbein *et al.*, 2006], may or may not have been continuous with slip on the main rupture at depth.)

Geodetic Observations

In addition to the postseismic creep observed along the main San Andreas trace, curious behavior of a continuous GPS site at Carr Hill is consistent with slip at depth working its way upward to manifest itself as creep on the main trace (Murray and Langbein, 2006). Carr Hill lies to the west of

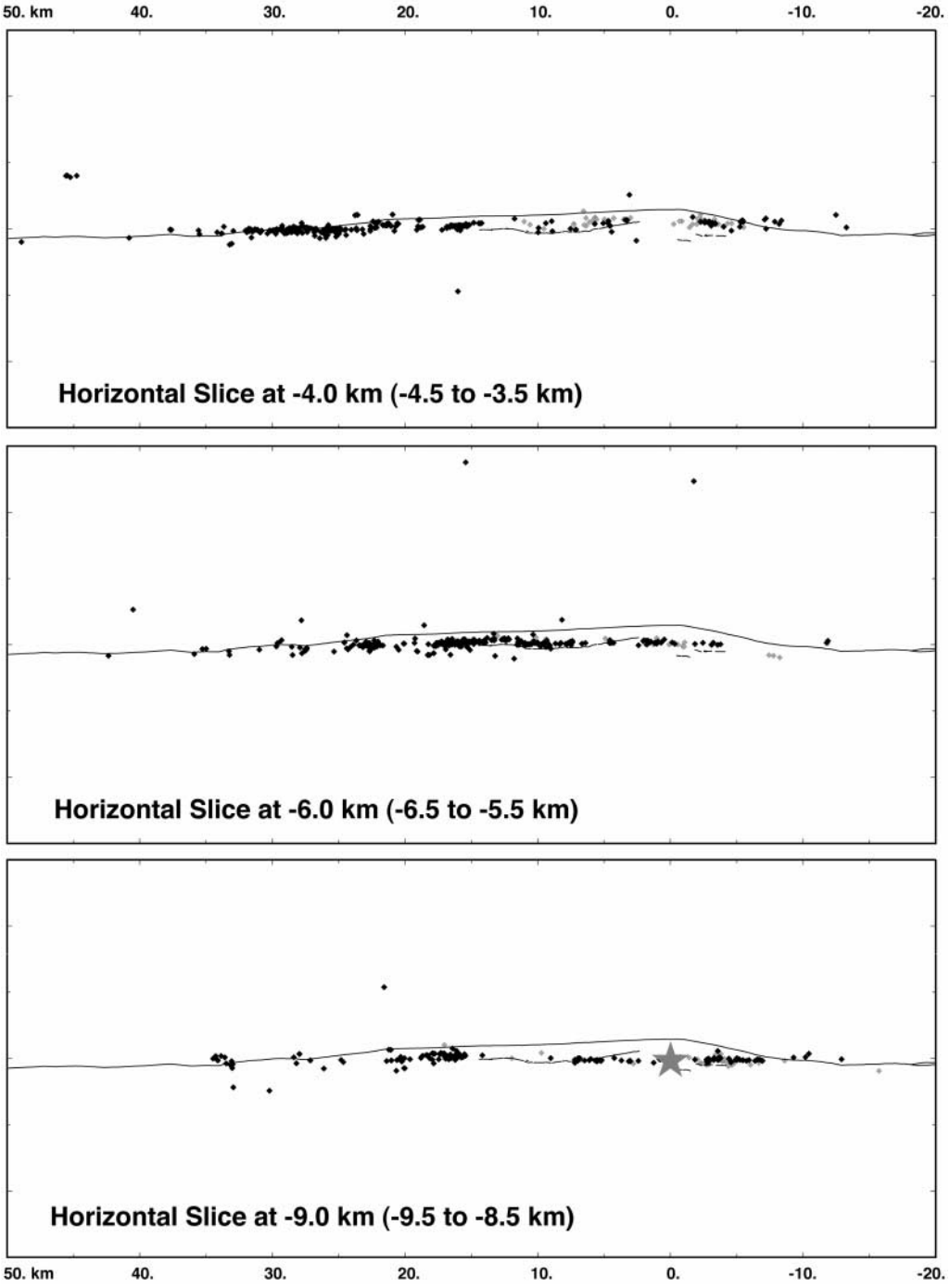

Figure 4. Map views of horizontal slices at 4-, 6-, and 9-km depth showing Parkfield aftershocks. The star represents the 2004 mainshock. Black dots are relocated 2004 aftershocks of Thurber *et al.* (2006); gray dots are 1966 relocated aftershocks (Bakun, 2005). Aftershocks shown for each slice are within ± 0.5 km of the central depth of the slice.

the mapped San Andreas trace so that its coseismic motion might have been expected to be to the northwest. In fact, it initially (coseismic plus two minutes of postseismic) moved to the southeast. Fitting this initial motion required slip on the deep coseismic rupture surface (which relocated aftershocks indicate lies to the southwest of Carr Hill), on the Southwest Fracture Zone, and on a surface connecting the rupture zone to the creeping main trace (Murray and Langbein, 2006). As time went on, the motion at Carr Hill reversed itself, and it began to move to the northwest as expected. It would appear that the fault strand that connects the rupture zone at depth with the creeping main trace must

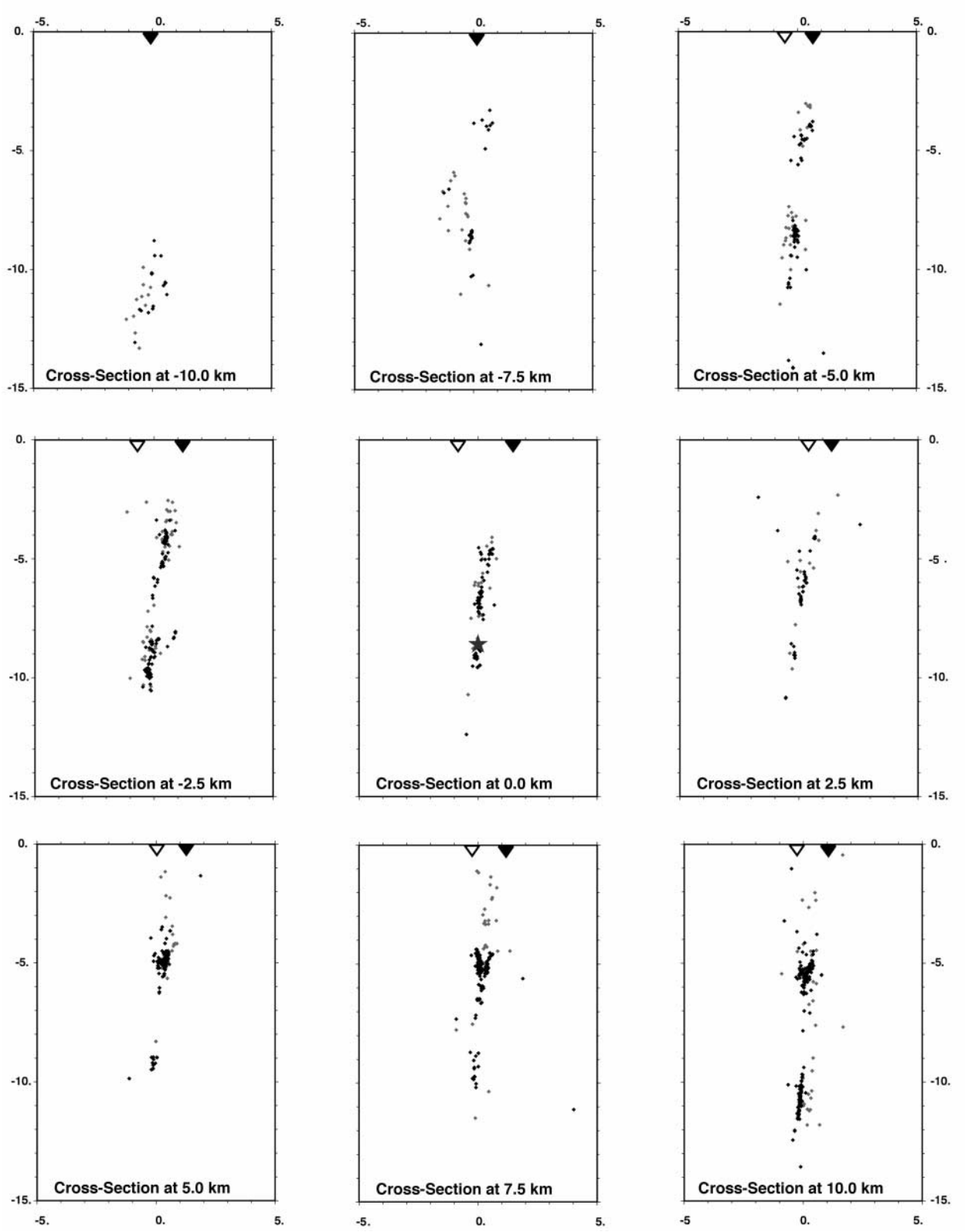

Figure 5. Cross-section views of Parkfield aftershocks. Vertical axis is depth in kilometers. Cross-section location is indicated by distance along strike from the 2004 hypocenter (see Fig. 4). The star on cross section at 0.0 km represents the 2004 mainshock. Black dots are relocated 2004 aftershocks of Thurber *et al.* (2006); gray dots are 1966 relocated aftershocks (Bakun, 2005). Aftershocks shown on each section are within ± 1.25 km of the center of the section along strike. Solid triangles show location of the main creeping San Andreas trace; open triangles show location of the Southwest Fracture Zone trace and Alquist–Priolo traces.

be a dipping surface that passes under Carr Hill, and that, as slip worked its way up this surface toward the Earth's surface, Carr Hill was gradually promoted to the correct side of the fault.

We hope that a careful analysis of existing geodetic data, which now span two complete Parkfield cycles (Murray and Langbein, 2006), may possibly reveal the warping process in action over time.

A Simple Dislocation Model

We constructed a simple elastic half-space dislocation model of the Parkfield region. (We assumed a Poisson's ratio of 0.25 and a shear modulus of 30 GPa.) Below 15 km, a single large (1000 × 1000 km) rectangular driving dislocation was forced to slip at a long-term slip rate of 35 mm/yr. Above, three layers of 100 5- × 5-km vertical rectangular dislocation patches filled the space between 0- and 15-km depth north of Cholame Valley. These patches were free to slip in response to changing stress produced by the deep driving dislocation, simulating the creeping zone north of Middle Mountain and the transitional zone between Middle Mountain and the south end of Cholame Valley that creeps aseismically and slips in frequent (relative to the repeat times of 1857-type earthquakes) **M** ~ 6 earthquakes. South of Cholame Valley, the fault between 0- and 15-km depth was held fixed, simulating the locked area of the fault that last ruptured in 1857. As slip at depth progresses, the originally straight fault plane becomes warped in map view forming a bulge to the northeast that tapers gradually toward the undeflected fault location to the northwest along strike. The southeast end of the bulge forms a more abrupt bend at the transition from slipping to locked patches across Cholame Valley, so that the general shape of the bulge in map view looks somewhat like the cross section of an airplane wing. We anticipate that the length of the bulge would be determined by both the locking depth (15 km here) and the material properties on the two sides of the fault.

Figure 2 shows in map view the horizontal displacement of a line (long dashed line) located 2.5 km northeast of the original straight dislocation fault, calculated after one million years of slip (with no intervening 1857-type events). The maximum calculated horizontal deformation rate perpendicular to the fault is approximately 4 mm/yr. In a perfectly elastic Earth, the entire warp would disappear after a repeat of the 1857 shock if stresses relaxed over the entire fault. However, the Earth is not a perfect elastic half-space (R. Wallace, personal comm., 1986), especially in its upper reaches, so that it seems unlikely that the warp in the fault will disappear entirely, even after a repeat of the 1857 event. By way of simple analogy, if one stretched a rubber band by an additional increment every year for many years and suddenly then released it, one would hardly expect it to return to its original length.

Slip on a warped surface might be expected to produce vertical deformation at the Earth's surface, and not surprisingly, if the simple dislocation model is forced to slip by 1 m in a right-lateral sense, the region encompassing Cholame Valley does subside (Fig. 6). We expect that geodetic deformation rates and long-term deformation expressed in topography will offer important constraints for future modeling efforts.

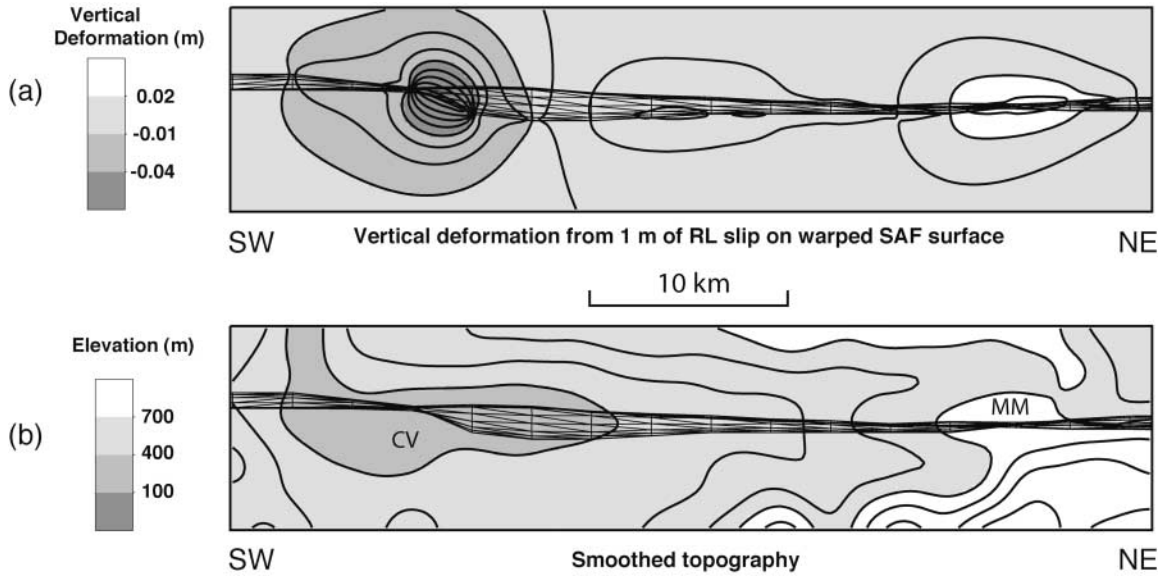

Figure 6. (a) Map view of vertical deformation in an elastic half-space predicted by 1 m of right-lateral slip in the simple dislocation model based on the warped surface shown in Figure 3. Contour interval is 0.01 m. (b) A smoothed representation of the topography in the Parkfield region. Contour interval is 100 m. CV, Cholame Valley; MM, Middle Mountain.

Finite-Element Models

We constructed a very simple finite-element model to test the idea of whether 1857-type earthquakes in a nonelastic medium could generate a growing eastward warp of the fault.

The model consists of a brick-shaped region forming a 300-km square in map view, 51 km deep. The fault is modeled as a vertical plane that runs in a north–south direction and bisects the region. There is a locked region on the fault, which occupies the southernmost 135 km of the fault at depths from 0 to 15 km. The locked region is allowed to rupture (i.e., slide without friction) once every 200 years, simulating an 1857-type earthquake. The rest of the fault is allowed to slide freely at all times. In this model, Cholame Valley is located at the point where the locked and freely sliding regions meet.

We constructed a finite-element mesh consisting of hexahedra. Near the fault, the elements are cubes 3 km on a side. Far from the fault, the elements are larger. All elements are quadratic (i.e, within each cell, displacement is approximated by a quadratic function of position).

To run the model, we first define the rheology. Then we drive the model by applying a right-lateral displacement to the eastern boundary of the model, relative to the western boundary of the model. The displacement is a steady 35 mm per year. Once every 200 years, the locked region is allowed to slide freely. Immediately after each simulated earthquake, we extract the surface trace of the fault and plot it.

If the rheology is perfectly elastic, then the fault trace returns to its initial position after each simulated earthquake. If the rheology includes viscoelastic or plastic materials, then there is a persistent distortion of the fault trace that grows with each earthquake cycle. In general, three cycles are sufficient to observe the trend.

We ran the model with several different rheologies. These rheologies are not intended to be realistic models of the rocks surrounding the San Andreas fault near Parkfield, nor are they intended to be an exhaustive set of possible rheologies. Therefore, these results must be regarded as merely exploratory and suggestive.

One rheology that yielded interesting results consists of three layers. From the surface to 6-km depth, the material is plastic. From 6- to 15-km depth, the material is elastic on the west side of the fault, and viscoelastic with a 50-year relaxation time on the east side of the fault. Below 15-km depth, the material is viscoelastic with a 200-year relaxation time. (The plastic material in the model is actually a mixture of plastic and elastic materials; the elastic admixture is needed to obtain numerical stability during fault rupture.) With this rheology, the fault trace bulged to the east, in a manner reminiscent of the San Andreas fault near Parkfield (although it does not match the San Andreas fault trace in detail). The maximum eastward deflection occurs at Cholame Valley, where the locked and freely sliding parts of the fault meet. The deflection tapers off gradually north of Cholame Valley, and more sharply south of Cholame Valley.

The use of rheology that differs on the two sides of the fault is intended to mimic the observed differences in the rocks on the two sides of the San Andreas fault. However, it is possible to obtain an eastward deflection using rheology that is the same on both sides of the fault. For example, if the previous rheology is modified so the region from 6- to 15-km depth is uniform (either all-elastic or all-viscoelastic), then there is still an eastward deflection of the fault. Given the crudeness of this model, it is impossible to say which option is the best fit to the observed shape of the San Andreas fault.

Interestingly, we also found some rheologies for which the fault warps to the west, which is opposite to what is observed at the San Andreas fault. One such rheology consists of two layers. From the surface to 6-km depth, the material is viscoelastic with a 50-year relaxation time. Below 6-km depth, the material is elastic. The result is a fault that warps westward everywhere except in the immediate vicinity of Cholame Valley. The fact that a change of rheology can alter not only the shape but also the direction of the fault warp suggests that observed fault geometry could convey information about the rheology of rocks near the fault. Future finite-element modeling may allow us to decide, for example, the degree to which the more competent sliver of gabbro at Gold Hill might have contributed to progressive curving of the fault trace through fault refraction around the more competent material.

Discussion

Rock units similar to those found at Gold Hill also exist at Logan Quarry near Hollister (Ross, 1984; Sims, 1993; Jachens *et al.*, 1998) about 180 km to the northwest. For slip rates on the San Andreas fault in the range of 35–25 mm/yr (Argus and Gordon, 2001; Titus *et al.*, 2005), and assuming that the Gold Hill and Logan Quarry rocks were once contiguous on the Pacific Plate, Gold Hill was probably dropped off at Parkfield about 5–7 Ma ago. A former San Andreas trace to the east of Gold Hill is approximately 5 km off the unwarped trend of the San Andreas, suggesting horizontal offset rates perpendicular to the San Andreas averaging about 1 mm/yr over the last 5–7 Ma. Given the simple dislocation model's warping rates of 4 mm/yr, Gold Hill's present location could be explained if approximately 15%–25% of the interseismic warping (between 1857-type events) in the near-surface materials were anelastic and not recovered at the times of 1857-type earthquakes (assuming that the active trace 5–7 Ma ago was already warped to a degree similar to the present active trace).

It will be noted that the previous discussion has assumed that the warp has been growing in the same place relative to Gold Hill for the last 5–7 Ma. If the explanation for the warp offered here is correct, it would imply that the locked patch to the south of Cholame Valley has remained stationary rela-

tive to Gold Hill and to the northeast side of the fault for this same period. If the locked patch and its accompanying warp had been moving northward or southward with time, the effects of warping on the northeast side of the fault might be expected to have been diluted (distributed) and to have left a longer but less distinctive wake.

There are many examples of warping or sinuosity (Bridwell, 1975) on strike-slip faults, although we are not aware of any examples as clearly defined as the Parkfield warp. The northern end of the central California creeping segment of the San Andreas fault lies near San Juan Bautista. The situation at this location is complicated by the intersection of the Calaveras fault and a restraining bend in the San Andreas as it passes through the Santa Cruz Mountains. The Calaveras fault provides another example of a sinuous, complex active trace at the Earth's surface underlain by a much simpler fault at depth as defined by relocated hypocenters (Simpson *et al.*, 2004). Judging from historic earthquakes and geodetic data along the Calaveras fault (Oppenheimer *et al.*, 1990; Manaker *et al.*, 2003), there are multiple locked patches along this fault capable of producing **M** $\sim$ 6 earthquakes, rather than the larger locked patch south of Cholame Valley capable of producing a **M** $\sim$ 8 event.

Our discussion so far has proposed a rather simple picture of the warping process while ignoring the considerable complexity that exists in the San Andreas fault zone at Parkfield. Near the San Andreas Fault Observatory at Depth (SAFOD) deep borehole, three flower structures have been identified across the fault zone, the most youthful near the current main trace, with a second older structure near the Southwest Fracture Zone and a third in between (Rymer *et al.*, 2004). Thayer and Arrowsmith (2005a,b) have described a major fault to the southwest of the current main trace near Middle Mountain that juxtaposes granitic rocks against Pinnacles–Neenach equivalent rocks, implying a fault jump to the northeast at some point rather than to the southwest as we have proposed. Sims (1993) suggests, however, that this jump occurred far to the south and the abandoned trace, now near Middle Mountain, was transported northward as part of the Pacific plate. If Sims is correct, this abandoned trace would have nothing to do with the warping process at Parkfield, although it does highlight that slicing and dicing in the fault zone is not uncommon (e.g., Swanson, 1989, 1990), especially in strike-slip faults that have not experienced much displacement (Wesnousky, 1988).

Our interpretation of the San Andreas fault geometry in the vicinity of Cholame Valley is somewhat at odds with the classic idea of a pull-apart rhombochasm located at a dilational step-over in a strike-slip fault, with the step-over extending to seismogenic depths (e.g., Reasenberg and Ellsworth, 1982). Recent improvements in earthquake relocation techniques suggest that, in a number of instances, strike-slip faults are simpler at depths below 5 km than one might infer from the geometry of surface traces or shallow seismicity (Graymer *et al.*, 2006). Parkfield may serve as an example of such behavior.

Conclusions and Speculations

The 50-km-long warp in the active San Andreas fault trace, from Cholame Valley on the southeast to beyond Middle Mountain on the northwest, may be a consequence of the locked patch south of Cholame Valley, which last ruptured in 1857 in the great **M** 7.9 Fort Tejon earthquake. The warp would be expected to grow over many 1857-type cycles until the geometry of the increasingly warped fault surface was no longer energetically favorable for strike-slip motion. More frequent **M** 6.0 Parkfield-type earthquakes may, by a similar nonelastic mechanism, add additional character to the shape of the warp.

The warp when viewed in three dimensions might be expected to diminish with depth. Its most extreme expression would be at shallower depths where rock materials might be expected to be most anelastic.

The geology to the northeast of the warp, including the exotic lithologies exposed at Gold Hill, suggests that bulging of San Andreas traces toward the northeast has been occurring in this vicinity for at least 5–7 Ma. This implies that the locked patch south of Cholame Valley may have remained fixed relative to the northeast side of the fault during this time, and that periodically, when the active surface of the fault becomes too deformed, slip is gradually transferred to a new straighter surface to the southwest. The former active trace is abandoned (and subsequently warped even more). The Southwest Fracture Zone, which lies approximately 1.5 km to the southwest of the current active fault, may be a potential successor to the present active trace, because it offers a straighter, less-deformed alternative for strike-slip motion.

The possibility that the Parkfield locked patch, which generates **M** $\sim$ 6 Parkfield events, has resulted from geometric complexities introduced by the warping needs to be explored. Perhaps large locked patches may be able to spawn smaller locked patches out in front of themselves by distorting a section of the adjacent fault surface that might otherwise be inclined to creep. Alternatively, exotic rocks left behind in the warped area when the fault periodically straightens itself may be stronger than the materials that they replace on the east face of the fault.

Irregularities in the traces of strike-slip faults may provide clues as to the location of locked patches or the rheologies of materials adjacent to the fault, or both. If inelastic behavior in upper crustal rocks is indeed the cause of these observed irregularities, the transition with depth from inelastic to (more) elastic behavior might be a favorable environment for the formation of subhorizontal detachment faults, given the temporally asymmetric nature of interseismic versus coseismic deformation.

The potential role of the Southwest Fracture Zone as a new straighter trace and the possibility of older traces still being able to carry slip suggest the importance of monitoring not just the current active trace. A truly integrated picture of the tectonics of the Parkfield region requires that we under-

stand how all of the various faults and fault strands are interacting and evolving in the short term and the long term.

Acknowledgments

Many thanks to Jim Lienkaemper and Carl Wentworth for assistance in obtaining fault traces in digital form. Thanks also to Jeanne Hardebeck and Felix Waldhauser for allowing us to use their relocated earthquake catalogs and for patiently supplying us with updated versions, and to Bob Jachens, Bill Stuart, and Carl Wentworth for sharing ideas. Ramon Arrowsmith, George Hilley, Paul Reasenberg, Jim Savage, and Rick Sibson provided helpful reviews.

References

Argus, D. F., and R. G. Gordon (2001). Present tectonic motion across the Coast Ranges and San Andreas fault system in central California, *Geol. Soc. Am. Bull.* **113,** 1580–1592.

Bakun, W. H., B. Aagaard, B. Dost, W. L. Ellsworth, J. L. Hardebeck, R. A. Harris, C. Ji, M. J. S. Johnston, J. Langbein, J. J. Lienkaemper, A. J. Michael, J. R. Murray, R. M. Nadeau, P. A. Reasenberg, M. S. Reichle, E. A. Roeloffs, A. Shakal, R. W. Simpson, and F. Waldhauser (2005). Implications for prediction and hazard assessment from the 2004 Parkfield earthquake, *Nature* **437,** 969–974.

Bridwell, R. J. (1975). Sinuosity of strike-slip fault traces, *Geology* **3,** 630–632.

Brown, R. D., Jr. (1970). Map showing recently active breaks along the San Andreas and related faults between the northern Gabilan Range and Cholame Valley, California, U.S. Geol. Surv. Misc. Invest. Map 1-575, scale 1:62,500.

Brown, R. D., Jr., J. G. Vedder, R. E. Wallace, E. F. Roth, R. F. Yerkes, R. O. Castle, A. O. Waananen, R. W. Page, and J. P. Eaton (1967). The Parkfield-Cholame, California, earthquakes of June–August 1966—Surface geologic effects, water-resources aspects, and preliminary seismic data, *U.S. Geol. Surv. Prof. Paper 579*, 66 pp.

Chinnery, M. A. (1966). Secondary faulting—I. Theoretical aspects, *Can. J. Earth Sci.* **3,** 163–190.

Dibblee, T. W., S. E. Graham, T. M. Mahony, J. L. Blissenbach, J. J. Mariant, and C. M. Wentworth (1999). Regional geologic map of San Andreas and related faults in Carrizo Plain, Temblor, Caliente and La Panza Ranges and vicinity, California: a digital database, *U.S. Geol. Surv. Open-File Rept. 99-14*, scale 1:125,000.

Dibblee, T. W., C. M. Wentworth, S. K. Brooks, K. M. Brown, S. E. Graham, R. S. Nicholson, and H. M. Wright (2004). Regional geologic map of San Andreas and related faults in the Priest Valley region, California, unpublished digital compilation, scale 1:125,000.

Dickinson, W. R. (1966). Structural relationships of San Andreas fault system, Cholame Valley and Castle Mountain Range, California, *Geol. Soc. Am. Bull.* **77,** 707–726.

Eaton, J. P., M. E. O'Neill, and J. N. Murdock (1970). Aftershocks of the 1966 Parkfield–Cholame, California earthquake: a detailed study, *Bull. Seism. Soc. Am.* **60,** 1151–1197.

Eberhart-Phillips, D., and A. Michael (1993). Three-dimensional velocity structure, seismicity, and fault structure in the Parkfield region, Central California, *J. Geophys. Res.* **98,** no. B9, 15,737–15,758.

Graymer, R. W., V. E. Langenheim, R. W. Simpson, R. C. Jachens, and D. A. Ponce (2006). Relatively simple through-going fault planes at large-earthquake depth may be concealed by surface complexity of strike-slip faults, in *Tectonics of Strike-Slip Restraining and Releasing Bends in Continental and Oceanic Settings*, P. Mann and D. Cunningham (Editors), *Special Volume of the Geological Society of London* (in press).

Jachens, R. C., C. M. Wentworth, and R. J. McLaughlin (1998). Pre-San Andreas location of the Gulalala Block inferred from magnetic and gravity anomalies, in *Geology and Tectonics of the Gualala Block, Northern California*, W. P. Elder (Ed.), Pacific Section SEPM, Book **84,** 27–64.

Jennings, C. W. (1977). Geologic map of California, Calif. Div. Mines Geol., Calif. Geol. Data Map Series, scale 1:750,000.

King, G., and J. Nabelek (1985). Role of fault bends in the initiation and termination of earthquake rupture, *Science* **228,** 984–987.

Langbein, J., J. R. Murray, and H. A. Snyder (2006). Coseismic and initial postseismic deformation from the 2004 Parkfield, California, earthquake, observed by Global Positioning System, Electronic Distance Meter, creepmeters, and borehole strainmeters, *Bull. Seism. Soc. Am.* **96,** no. 4B, S304–S320.

Lienkaemper, J. J., B. Baker, and F. S. McFarland (2006). Surface slip associated with the 2004 Parkfield (CA) earthquake measured on alinement arrays, *Bull. Seism. Soc. Am.* **96,** no. 4B, S239–S249.

Lindh, A. G., and D. M. Boore (1981). Control of rupture by fault geometry during the 1966 Parkfield earthquake, *Bull. Seism. Soc. Am.* **71,** 95–116.

Manaker, D. M., R. Burgman, W. H. Prescott, and J. Langbein (2003). Distribution of interseismic slip rates and the potential for significant earthquakes on the Calaveras fault, central California, *J. Geophys. Res.* **108,** no. B6, 2287, doi 10.1029/2002JB001749.

McPhee, D. K., R. C. Jachens, and C. M. Wentworth (2004). Crustal structure across the San Andreas Fault at the SAFOD site from potential field and geologic studies, *Geophys. Res. Lett.* **31,** L12S03, doi 10.1029/2003GL019363.

Murray, J., and J. Langbein (2006). Slip on the San Andreas fault at Parkfield, California, over two earthquake cycles: implications for seismic hazard, *Bull. Seism. Soc. Am.* **96,** no. 4B, S283–S303.

Oppenheimer, D. H., W. H. Bakun, and A. G. Lindh (1990). Slip partitioning of the Calaveras Fault, California, and prospects for future earthquakes, *J. Geophys. Res.* **95,** no. B6, 8483–8498.

Reasenberg, P., and W. L. Ellsworth (1982). Aftershocks of the Coyote Lake, California, Earthquake of August 6, 1979: a detailed study, *J. Geophys. Res.* **87,** B13, 10,637–10,655.

Ross, D. C. (1984). Possible correlations of basement rocks across the San Andreas, San Gregorio–Hosgri, and Rinconada-Reliz–King City faults, California, *U.S. Geol. Surv. Prof. Paper 1317*, 97 pp.

Rymer, M. J., R. D. Catchings, M. Thayer, and J R. Arrowsmith (2004). Structure of the San Andreas fault zone and SAFOD drill site as revealed by surface geologic mapping and seismic profiling near Parkfield, California, *EOS Trans. Am. Geophys. Union* **85,** no. 47, Fall Meet. Suppl., Abstract T11F-08.

Rymer, M. J., J. C. Tinsley, J. A. Treiman, J R. Arrowsmith, K. B. Clahan, A. M. Rosinski, W. A. Bryant, H. A. Snyder, G. S. Fuis, N. Toké, and G. W. Bawden (2006). Surface fault slip associated with the 2004 Parkfield, California, Earthquake, *Bull. Seism. Soc. Am.* **96,** no. 4B, S11–S27.

Segall, P., and D. D. Pollard (1980). Mechanics of discontinuous faulting, *J. Geophys. Res.* **85,** 4337–4350.

Sibson, R. H. (1986). Rupture interaction with fault jogs, in *Earthquake Source Mechanics*, S. Das, J. Boatwright, and C. H. Scholz (Editors), American Geophysical Monograph 37, 157–167.

Sieh, K. (1978). Slip along the San Andreas fault associated with the great 1857 earthquake, *Bull. Seism. Soc. Am.* **68,** 1421–1448.

Simpson, R. W., R. W. Graymer, R. C. Jachens, D. A. Ponce, and C. M. Wentworth (2004). Cross-sections and maps showing double-difference relocated earthquakes from 1984–2000 along the Hayward and Calaveras Faults, California, *U.S. Geol. Surv. Open-File Rep 2004-1083,* Version 1.0, http://pubs.usgs.gov/of/2004/1083/ (last accessed July 2006).

Sims, J. D. (1993). Chronology of displacement on the San Andreas fault in central California: evidence from reversed position of exotic rock bodies near Parkfield, California, in *The San Andreas Fault System: Displacement, Palinspastic Reconstruction, and Geologic Evolution*, R. E. Powell, R. J. Weldon, II, and J. C. Matti (Editors). *Geol. Soc. Am. Memoir* **178,** 231–256.

Swanson, M. T. (1989). Sidewall ripouts in strike-slip faults, *J. Struct. Geol.* **11,** no. 8, 933–948.

Swanson, M. T. (1990). Extensional duplexing in the York Cliffs strike-slip fault system, southern coastal Maine, *J. Struct. Geol.* **12,** no. 4, 499–512.

Thayer, M. R., and J R. Arrowsmith (2005a). Fault zone structure of Middle Mountain, Central California, *EOS Trans. Am. Geophys. Union*, **86,** no. 52, Fall Meet. Suppl., Abstract T21A-0458.

Thayer, M. R., and J R. Arrowsmith (2005b). Geology and geomorphology of the San Andreas fault near Parkfield, California, geologic mapping and structural synthesis, http://activetectonics.la.asu.edu/Parkfield/structure.html (last accessed July 2006).

Thayer, M. R., R. Arrowsmith, J. Young, A. Fayon, and M. Rymer (2004). Geologic structure of Middle Mountain within the San Andreas fault zone near Parkfield, *EOS Trans. Am. Geophys. Union* **85,** no. 47, Fall Meet. Suppl., Abstract T13A-1335.

Thurber, C., H. Zhang, F. Waldhauser, J. Hardebeck, A. Michael, and D. Eberhart-Phillips (2006). Three-dimensional compressional wavespeed model, earthquake relocations, and focal mechanisms for the Parkfield, California, region, *Bull. Seism. Soc. Am.* **96,** no. 4B, S38–S49.

Titus, S. J., C. DeMets, and B. Tikoff (2005). New slip rate estimates for the creeping segment of the San Andreas fault, California, *Geology* **33,** 205–208.

Wesnousky, S. G. (1988). Seismological and structural evolution of strike-slip faults, *Nature* **335,** no. 6188, 340–343.

U.S. Geological Survey
345 Middlefield Road, MS 977
Menlo Park, California 94025
(R.W.S., J.L., J.R.M., M.J.R.)

Invisible Software
San Jose, California
(M.B)

Manuscript received 23 September 2005.